

THERMAL ANALYSIS OF MOROCCAN PHOSPHATES 'YOUSOUFIA' IN AN OXIDATIVE ATMOSPHERE BY TG AND DSC

A. Aouad, M. Benchanâa , A. Mokhlisse and A. Ounas*

Laboratoire de Chimie-Physique, Faculté des Sciences Semlalia, Université Cady Ayyad, BP: 2390,
40001 Marrakech, Maroc

(Received June 23, 2003; in revised form November 24, 2003)

Abstract

A non-isothermal experimental study using thermogravimetry (TG) and differential scanning calorimetry (DSC) was conducted for investigation the oxidation reactivity of natural phosphate and its demineralised products. The analyses were carried out in oxygen atmosphere and at different heating rate (5, 10, 20, 30, 50, 60°C min⁻¹) up to 1000°C. The results indicated that the material washed with HCl from the original phosphate, mainly apatite and carbonates of calcium and magnesium, as well as with HCl/HF, silicates minereals, had an inhibition effect during oxidation reactions of organic material. The increase of the heating rate shifted the reactions to higher temperatures. In addition, kinetic parameters were determined by assuming a single first-order kinetic model, using the Coats–Redfern method. The influences of demineralization process of natural phosphate and the heating rate were examined and discussed.

Keywords: demineralization, DSC, kerogen, kinetics, natural phosphate, oxidation, TG

Introduction

Natural phosphate consists of complex organic material of high molecular mass called kerogen, which is finely distributed, in an inorganic matrix [1]. The inorganic constituent of the natural phosphate affects the reactions of the organic matter both physically and chemically. The interaction between kerogen and the inorganic matrix during oxidation reactions during the calcination process is not well understood. The basic principles of the oxidation mechanism of phosphate may be understood by examining the overall oxidation behaviour of the original phosphate and taking into consideration the interaction between kerogen and the inorganic matrix. The oxidation behaviour of the demineralization products provides useful information on the interaction between the kerogen and inorganic matrix of the natural phosphate.

In other hand, the factors controlling the heterogeneous kinetics of reactions involving a solid phase are inadequately understood. Reaction of the solid particle with a

* Author for correspondence: E-mail: benchanaa@ucam.ac.ma

reactive gaz starts at the surface where the reactants contact. The interaction of a solid particle with a reactive gaz theoretically involves: (a) the diffusion of the gas to the surface and into the pores of the solid particle; (b) diffusion from the particle surface or from the pores into the reaction sites and (c) reaction between the gas and the solid. The effect of penetration will be more or less marked depending on the relative rates of reaction and diffusion [2]. The overlapping of these stages depends on number of factors, some related to the operating conditions (heating rate, pressure, temperature...) and others to the sample properties (pore structure, surface area, particle size...) [3].

The purpose of the present study is to obtain some basic information on the non-isothermal combustion (oxidation) of the natural phosphate and to discuss the effects of the demineralization process, physical and chemical changes, and the heating rate during oxidation reactions of organic material. The study is based on non-isothermal oxidation experiments under an oxidative atmosphere using thermogravimetric and DSC techniques.

Experimental

Samples

Phosphate samples were obtained from a mine located at Youssoufia (Western Morocco). Rock phosphates in this site cover an area of about 700 km², which extends over 50 km in length. The phosphate bed has a maximum depth of 15 m and is divided into layers II–III and I deposited during the Montien and Maestrichien periods, respectively. Our samples are from layer I where the organic matter is trapped in the framework of the rocks. Favourable physical conditions allowed the conversion of this matter to bituminous compounds, responsible for the grey colour of the phosphate [4].

Preparation of kerogen

The natural phosphate and its demineralized products obtained by HCl and HF washings, carbonate-free-phosphate (CFP) and silicate-free-phosphate (kerogen), respectively, were used in this study. The natural phosphate was demineralized to the concentrated kerogen with HCl and HF by a method previously described [5]. 100 g of dried natural phosphate were treated with chloroform to extract the bitumens until the solvent in the Soxhlet arm becomes colourless. The bitumen-free phosphate (BFP) was then dried and weighed. It is subsequently attacked with HCl until no further carbon dioxide evolved. The residue was washed with hot distilled water until the silver nitrate test for chlorides was negative. The hydrochloric attack was repeated twice to eliminate all calcium products. CFP was dried, washed with concentrated HCl and treated with concentrated HF (5 mL/(g of CFP)) at 60°C under a nitrogen atmosphere for 8 h. The silicate-free phosphate obtained in this step was then washed with hot distilled water and the HF treatment step was repeated. After drying the silicate-free phosphate, a saturated boric acid solution was added and the sample was stirred for 30 min. Finally, the remaining brown solid was treated with 6 M HCl and the kerogen was washed with hot distilled water to remove chlorides and dried overnight at 60°C. It should be noted

that pyrite is known to be the major mineral component remaining after HCl/HF treatment [6]. The yields of the demineralization procedure and elemental analyses are presented, respectively, in Table 1 and Table 2.

Table 1 The composition of natural phosphate

Component	Composition/mass%
Bitumen	0.40±0.03
Apatite, carbonates ^a	86.60±0.20
Silicates	7.90±0.10
Pyrite	0.30±0.01
Kerogen	4.80±0.10

^aIncludes sulphides, sulphates, oxides and hydroxides.

Table 2 Elemental analyses of the natural phosphates and its kerogen

Element/mass%	C/%	H/%	S/%	N/%	O/%
Natural phosphate	67.5	7.6	11.1	2.1	11.7
Kerogen	68.1	7.2	9.5	3.0	12.2

Analyses

The process of oxidation was followed using a Rheometric Scientific Model-STA 1500. The analyzer combines a sensitive thermogravimetric balance with a heat-flux DSC handing down for simultaneous DSC and TG experiments. The sample mass loss and heat flow during the course of the reaction have been continuously recorded as a function of temperature and time. The samples of between 7 and 10 mg were heated under oxygen atmosphere (100 mL min⁻¹) from 25 to 1000°C at various heating rates. We have not been able to treat kerogen with heating rates higher than 5°C min⁻¹ because of the great reactivity of this latter with oxygen. The X-ray diffractograms were obtained with a Philips diffractometer using the CuK_α radiation produced at 32 kV and 20 mA by a Philips PW 1043 X-ray tube. The surface areas of the natural phosphate and its demineralized products were measured by the nitrogen adsorptive method at 77 K.

Results and discussion

Thermogravimetric analysis

Figure 1 represents the mass loss data for natural phosphate as a function of temperature at various heating rates to a final oxidation temperature of 1000°C in oxygen atmosphere. The figure indicates that natural phosphate exhibited distinct steps of thermal oxidation as the temperature was increased.

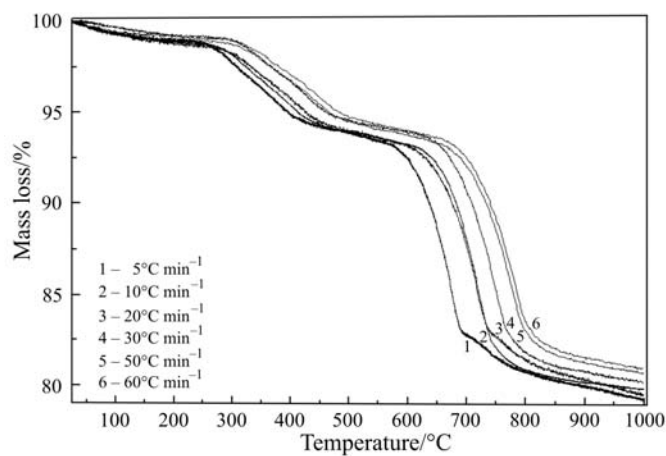


Fig. 1 Non-isothermal TG curves at different heating rates in oxygen for natural phosphate

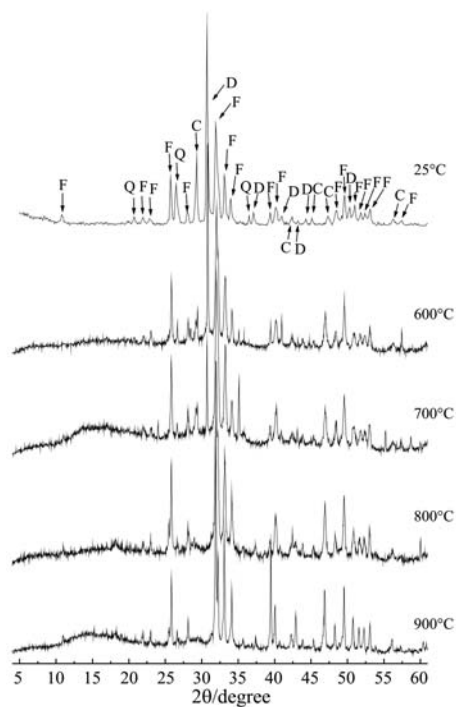


Fig. 2 X-ray diffractogram for sequential pyrolysis of the natural phosphate
F – fluorcarbonateapatite, D – dolomite, C – calcite, Q – quartz

Lower temperature thermal oxidation, of about 170°C produced mass loss, which was attributed to the loss of moisture. The mass loss, from about 170 to 600°C, is due to loss of hydrocarbon materials. Mass loss of this part represents about 5% of the total nat-

ural phosphate mass. The natural phosphate exhibited a one-step thermal oxidation in the main mass loss and is attributed to hydrocarbon volatile formation that is, in the temperature range of 180–600°C, suggesting a one-step evolution of hydrocarbon volatile from the phosphate. The one-step decomposition was also observed in a previous TG/DGA study in inert atmosphere [5]. Heating above 600°C produced carbonate decomposition at a temperature between 600 and 800°C due to the presence of the carbonate minerals such as calcite and dolomite present originally in natural phosphate. This result is supported by the X-ray diffraction study of the natural phosphate treated at different temperatures shown in Fig. 2. This figure shows the progressive reduction (X-ray diffractograms at 600 and 700°C) and the complete disappearance (X-ray diffractograms at 800 and 900°C) of the peaks characteristic of calcite and dolomite. This caused a mass loss of about 16% of the total natural phosphate mass.

Table 3 Comparison of thermogravimetric data in relation to heating rate and phosphate products

Sample	$\beta/^\circ\text{C min}^{-1}$	Mass loss/%		
		180–550°C	550–1000°C	Total
Natural phosphate	5	5.04	14.63	20.73
	10	5.10	14.51	20.81
	20	4.84	14.54	20.46
	30	4.63	13.83	19.72
	50	4.61	13.58	19.29
	60	4.53	13.24	18.98
Free-carbonate-phosphate	5	46.76	3.11	52.84
	10	46.70	3.01	52.30
	20	46.69	2.89	51.84
Kerogen	30	46.52	2.68	50.60
	5	89.8	5.01	94.81

Table 3 shows the data of mass loss in the medium and high temperature regions in relation with the heating rate in terms of mass loss percentage. The table emphasizes the significant difference concerning the effect of heating rate on total mass loss. As the heating rate increased, the total mass loss decreased. This difference is due to the shorter exposure time to a particular temperature at a faster heating rate. It was also observed that higher rates resulted in higher reaction temperatures.

DSC analysis

It is well known that the DSC technique is used to enable one to follow the changes in heat flow during the history of reactions. The heat flow may be from the reaction exothermic or to the source of the reaction endothermic or a mix of them. Figure 3 shows some representative DSC curves for the natural phosphate and corresponding demineral-

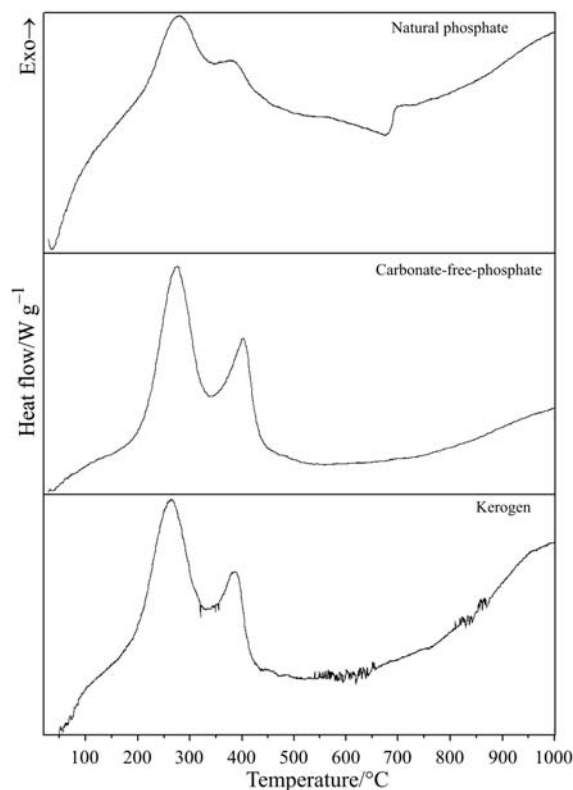


Fig. 3 DSC curves at heating rate of $5^{\circ}\text{C min}^{-1}$ in oxygen for phosphate products

ized products, for a heating rate of $5^{\circ}\text{C min}^{-1}$ up to 1000°C in an oxygen atmosphere. It is seen from the figure that all DSC curves exhibited mainly an endothermic peak started at 30 and ended at 150°C due to the evaporation of moisture water and two exothermic peaks at 282 and 381°C . As they occurred in the DSC curve of kerogen concentrate, these peaks were the result of the oxidation of only the organic matter in the original phosphate. This temperature portion of the thermal curves presented thermal decomposition identical to that observed in inert atmosphere. Moreover, it has been shown by FTIR spectroscopy technique on the residues after each stage of pyrolysis that the two major DSC peaks pyrolysis denoting a two-stage pyrolysis (combustion) of the kerogen components; the first one involved the complete decomposition of aliphatic constituents whereas the second one was the pyrolysis of an aromatic residue [7].

Similar results were obtained by other workers using DTA and DSC to investigate the oxidation of oil shales and coals [8–11]. In this regard, Stuart *et al.* [12] suggested that the two oxidation peaks correspond to two types of organic materials, which were pyrolysed at distinct temperatures, while Cetinkaya *et al.* [10] attributed these peaks to the chain oxidation reactions of the type of material in the organic matrix.

At the DSC curve of natural phosphate two unresolved endothermic effects above 600°C, caused by decomposition of carbonate minerals, have disappeared from its demineralized products. The first endothermic peak between 600 and 750°C corresponds to the decomposition of dolomite, between 750 and 840°C due to the decomposition of calcite (Fig. 4, line 6) [13].

At a temperature above 800°C, incomplete exothermic peak is observed in phosphate product experiments (Fig. 3). This could be a consequence of the secondary ox-

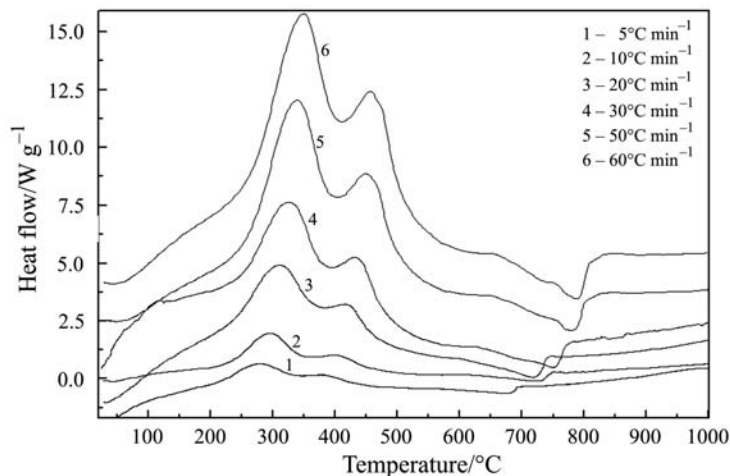


Fig. 4 DSC curves at different heating rates in oxygen for natural phosphate

idation of residual carbon produced during kerogen degradation. It is clear that the observed effect could not be related to the oxidation of mineral phosphates, because the same effect did not appear with an increase of the heating rate during the oxidation of natural phosphate (Fig. 4).

Because of the difference in physical (i.e., porosity, surface area) and chemical (i.e., mineral matter content) properties, the DSC curves of combustion of natural phosphate and its demineralized exhibited significant variations. The characteristic parameters related to these peaks such as the initial temperature of kerogen oxidation (T_{onset}), temperature of maximum heat flow (T_{m1} , T_{m2} , T_{m3}) and combustion heats of both organic (ΔH_1) and the inorganic (ΔH_2) components of the natural phosphate in relation to the heating rate for each phosphate product are listed in Table 4. The examination of these values indicates that T_{onset} of kerogen oxidation is lower in kerogen concentrate than in the corresponding raw phosphate and decarbonated phosphate at about 20 and 30°C, respectively. A lower T_{onset} may be as result of a higher reactivity for the sample-oxygen reaction [14]. These observation suggest that the reactivity order for T_{onset} of natural phosphate and its demineralized products as follows:

kerogen>decarbonated phosphate>original phosphate.

Table 4 Comparison of DSC data in relation to phosphate products

Samples	$\beta/^\circ\text{C min}^{-1}$	Temperature/ $^\circ\text{C}$				Heat of combustion/ kJ mol^{-1}	
		T_{onset}	T_{m1}	T_{m2}	T_{m3}	ΔH_1	ΔH_2
Natural phosphate	5	205	282	381	677	-1.97	0.44
	10	217	296	402	700	-1.86	0.37
	20	228	309	415	718	-1.60	0.26
	30	237	327	432	749	-1.56	0.21
	50	250	339	449	779	-1.41	0.12
	60	252	350	456	788	-1.39	0.13
Free-carbonate-phosphate	5	193	274	402	-	-16.60	-
	10	205	288	415	-	-15.80	-
	20	212	297	430	-	-15.00	-
	30	226	312	443	-	-14.80	-
Kerogen	5	176	165	385	-	-34.43	-

This may be due to the demineralization process, which changed the surface area of the natural phosphate (Table 4) and the diffusion of oxygen into the phosphate matrix might be enhanced, and this could influence the temperature of the oxidation reactions. The physical changes are not the only factor of low T_{onset} of kerogen oxidation. However, the decrease in the T_{onset} may be a consequence of the adsorptive effect of the mineral matter, which might retain a part of the generated hydrocarbon in the samples containing mineral matter [11].

Similarly to T_{onset} , the first maximum heat flow temperature (T_{m1}) may also be used to comparing the reactivity of the samples [15, 16]. Phosphate combustion is a heterogeneous reaction and the rate of heat flow is a function of the combustion rate. A lower temperature for the maximum heat flow is a consequence of the higher combustion rate. Based on this fact, the temperature of the maximum heat flow given in Table 4 may be used to define of a new reactivity order. These findings clearly show that the demineralization process caused a dramatic decrease in T_{onset} as well as T_{m1} temperatures. But, the second maximum heat flow temperature (T_{m2}) increases as the demineralization process was performed. This result is in agreement with those obtained by Yürüm *et al.* [17] during the oxidation of oil shales and its demineralized products. No explanation was given by these authors for the interpretation of this difference in temperature.

As the heating rate is increased, there is a shift to higher temperatures for the T_{m1} , T_{m2} and T_{m3} . The shift in the DSC peaks is illustrated in Figs 4 and 5. This can be attributed to the variations in the heat transfer rate with the change in the heating rate and the short exposure time to a particular temperature at the higher rates [18], as well as the effect of the kinetics of oxidation [19]. At higher heating rates, the surface of each phosphate particle will be at higher temperatures than that of its core. This

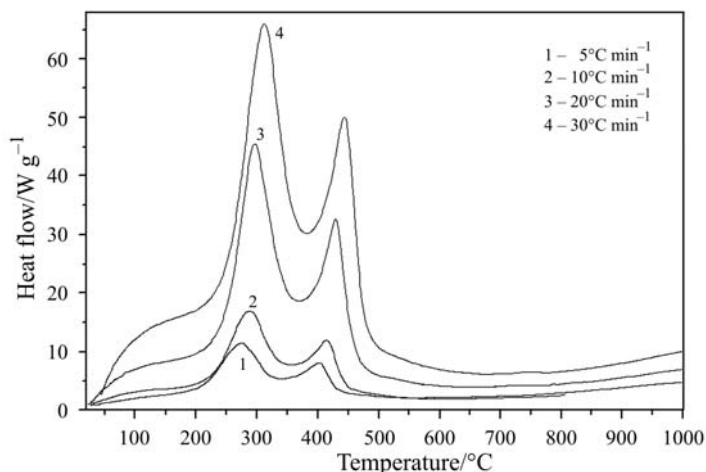


Fig. 5 DSC curves at different heating rates in oxygen for CFP

would lead to reactions occurring inside the particle at a relatively low temperature and the resulting products passing through the higher temperature region, hence, secondary reactions ensue before emission from the particle. These secondary reactions reduce the yield of phosphate product [20]. This result is in accordance with the TG data discussed earlier.

The effect of heating rate in the combustion heat of both organic (ΔH_1) and the inorganic (ΔH_2) components of the natural phosphate and its demineralized products is indicated in Table 4. The increase of heating rate decreased the heat of combustion of both organic matter and the mineral matrix in phosphate product. Moreover, comparisons of these energy values for the combustion reactions of the organic materials (ΔH_1) and mineral materials (ΔH_2) clearly show that the energies generated from the combustion of organic matter are higher than those of the mineral materials. Their heats of combustion range between -1.4 and -2 kJ g^{-1} and 0.1 and 0.5 kJ g^{-1} , respectively. These findings suggest that the organic compounds in raw phosphate is beneficial, providing an additional source of energy.

Kinetic approaches

Thermogravimetric data

The use of TG to determine kinetic parameters for the thermal process (pyrolysis or oxidation) for solid fuels is extremely complicated, because of the presence of a complex mixture of kerogen and a wide range of minerals. In addition, their devolatilisation presents a large number of reaction in parallel and series whilst the TG provides general information on the overall reaction kinetics rather than individual reactions and therefore the activation energies derived from TG should be termed apparent activation energies. However, the technique has been used in several researches and gave useful comparative data and was used in this work to examine the influence of demineralization process and heating rate on the apparent activation energies in oxi-

dation process of natural phosphate. The approach adopted by many workers in the kinetic of TG data for a variety of materials is to assume [21, 22] or to determine [23, 24] a first-order rate of reaction for the process of devolatilisation. Similarly, the approach adopted here is to assume a first-order reaction with respect to the amount of undecomposed materials and that the sample size is enough small to eliminate heat transfer effects.

TG involves a non-isothermal analysis of solids fuels, whereas most kinetic data is derived from isothermal studies. In isothermal analysis, the rate of reaction is determined at a constant temperature, whilst in non-isothermal studies, time and temperature are coupled via a constant heating rate. The non-isothermal TG technique has been preferred by some researchers [21–25] because of its advantages over the isothermal method. These advantages include: the elimination of errors due to the thermal induction period; it also permits a rapid scan of the whole temperature range of interest; and it also simulates conditions expected in large scale retorting processes more closely.

There are several approaches to the kinetic analysis of thermogravimetric data to determine the kinetic parameters for the thermal degradation of sample [21, 24, 26, 27]. The approach adopted in this work was the mathematical equation developed by Coats and Redfern [28] for the non-isothermal analysis of thermogravimetric data.

$$\frac{1-(1-\alpha)^{1-n}}{(1-n)T^2} = \left(\frac{AR}{\beta E}\right) \left(\frac{1-2RT}{E}\right) \exp\left(\frac{-E}{RT}\right) \quad (1)$$

where α is the fraction decomposed, T is absolute temperature (K), n is the overall reaction order, E is the apparent activation energy (kJ mol^{-1}), A is the pre-exponential factor, R is the gas constant ($\text{kJ mol}^{-1} \text{K}^{-1}$) and β is the heating rate ($^{\circ}\text{C min}^{-1}$).

Equation (1) may be further simplified if we assume $2RT \ll E$. Based on these assumptions, the following equation may be used to estimate the kinetic parameters from TG data:

$$\ln\left[\frac{1-(1-\alpha)^{1-n}}{(1-n)T^2}\right] = \ln\left(\frac{AR}{\beta E}\right) - \frac{E}{RT} \quad (2)$$

With some assumptions, the integral of Eq. (1) for the first-order reaction ($n=1$) gives:

$$\ln\left[-\frac{\ln(1-\alpha)}{T^2}\right] = \ln\left(\frac{AR}{\beta E}\right) - \frac{E}{RT} \quad (3)$$

The plot of $\ln[-\ln(1-\alpha)/T^2]$ vs. $1/T$ corresponding to a straight line with a slope of $-E/R$ can be used to evaluate the activation energy. The pre-exponential factor can be determined from the intercept.

Figure 6 shows that the first-order reaction model generally gives a straight line with higher correlation coefficients (R) for each heating rate. Therefore, the assumption related to the first-order is valid for the temperature region below 600°C . The variation in heating rate did not alter the slopes of these lines. Moreover, the influ-

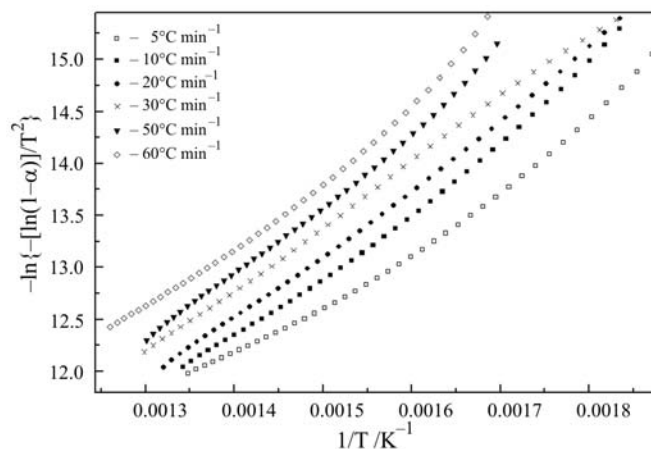


Fig. 6 Determination of kinetic parameters from TG data for different heating rates for natural phosphate

ence of heating rate on the activation energies was not clear, it was very similar irrespective of heating rate.

The apparent activation energies for natural phosphate and its demineralized products in relation to heating rate are shown in Table 5. An activation energy is represented for the phosphate products corresponding to the one-step of TG experiments for the main region temperature. There is a significant decrease in apparent activation energy with the removal of the mineral matrix. Balice *et al.* have suggested that the diffusion of the organic matter throughout the mineral matrix required a higher temperature and relatively more energy [29]. This is in accordance with the greater T_{onset} observed for original phosphate. This finding is consistent with the results reported by Dembick [30]. This latter concluded that added mineral matter such as quartz, calcite and dolomite shifted the activation energy to values higher than observed for the isolated kerogen. This therefore suggests that the increase of the apparent activation energy is a consequence of the adsorptive effect of the mineral matter, which might retain a part of the generated hydrocarbon in the samples containing mineral matter.

The mineral matter content is not the only factor of low activation energies. However, the decrease in the activation energy may be a consequence of the physical structure of the solid during the demineralization process. After the acid treatments, porosity, and total surface area increased as almost all of the inorganic matter of original phosphate is removed (Table 6). The surface area of solid fuels plays an important role in combustion. Oxygen must enter the pore mouths and penetrate into the particle. The oxidation occurs at the surface of the pores. Thus, the reactivity is proportional to the surface area and pore distribution. The transfer of oxygen molecules into the pore surface and the transfer of the product back to the gas phase are easier for larger pores. However, there is a decrease with an increase of the surface area of the phosphate products. Similar results were reported by other authors [31–33]. Weitkamp and Gutberlet [34] suggested that apparent activation energies should rise as the effects of diffusion processes in thermal treatment of oil shales are reduced.

Table 5 Kinetic parameters determined using the Coats–Redfern method

Samples	Natural phosphate					Free-carbonate-phosphate					Kerogen	
	5	10	20	30	50	60	5	10	20	30		5
$\beta/^\circ\text{C min}^{-1}$	47.06	53.79	52.73	50.28	54.77	52.33	39.21	41.89	38.8	42.6	34.65	5
$E/\text{kJ mol}^{-1}$	1.93	1.87	6.26	8.87	24.21	9.13	2.89	2.72	6.94	4.60	2.69	2.69
$A/10^{-6} \text{ min}^{-1}$	0.993	0.998	0.997	0.997	0.999	0.995	0.996	0.989	0.994	0.998	0.997	0.997

*Correlation coefficient

Table 6 Surface area analyses of phosphate products

Samples	Surface area/m ² g ⁻¹
Natural phosphate	3.15
Free-carbonate-phosphate	8.25
Kerogen	15.18

Conclusions

The conclusions of this work are summarised as follows:

- The combustion of natural phosphate in simultaneous TG/DSC showed distinctly thermal oxidation depending on the heating rate. There was a shift in maximum heat flow of DSC curves to higher temperatures as the heating rate was increased.
- The combustion reactivity of natural phosphate was affected by the chemical and physical changes caused during demineralization process.
- Kinetic parameters, for main temperature region 180–600°C, were determined by assuming a single first-order kinetic model, using the integral method for TG analysis.
- The examination of kinetic parameters of natural phosphate and its demineralized products clearly showed that the demineralization process caused a decrease in the activation energy.

* * *

The authors wish to express their tanks to Professors G. Bertrand and J. P. Bellat (Laboratoire de Recherche sur la Réactivité des Solides, Faculté des Sciences Mirande – Dijon, France) for their help during this work which was performed in the framework of Franco-Moroccan (University Cady Ayyad, Marrakech – University of Bourgogne and Regional Council, Dijon) cooperation. It has also benefited from the support of the Direction of the Mining Exploration of Gantour at Youssoufia. We kindly thank these organisms.

References

- 1 Benalioullhaj, Thesis, University of Louis Pasteur, Strasbourg, France 1991.
- 2 R. E. Essenhigh, in M. A. Iliott (Ed.), Chemistry of coal utilization, Wiley, New York 1981, p. 1153.
- 3 D. L. Smoot, Prog. Energy Combust. Sci., 10 (1984) 229.
- 4 M. Zayad, M. Khaddor and M. Halim, Fuel, 72 (1993) 655.
- 5 A. Aouad, L. Bilali, M. Benchanâa and A. Mokhlisse, J. Therm. Anal. Cal., 67 (2002) 733.
- 6 B. Durand and G. Nicise, in: B. Durand (Ed.), Kerogen, Edition Technip, Paris 1980, p. 35.
- 7 A. Aouad, M. Benchanâa, A. Mokhlisse, M. Elhaddek and A. Aarafan, J. Therm. Anal. Cal., 70 (2002) 593.
- 8 D. Skala, S. Korica, D. Vitorovic and H. J. Neumann, J. Therm. Anal. Cal., 49 (1997) 745.
- 9 M. V. Kök and M. R. Pamir, J. Therm. Anal. Cal., 53 (1998) 567.
- 10 S. Cetinkaya and Y. Yürüm, Fuel Process. Technol., 67 (2000) 177.

- 11 A. G. Borrego, J. G. Prado, E. Fuente, M. D. Guillén and C. G. Blanco, *J. Anal. Appl. Pyrol.*, 56 (2000) 1.
- 12 W. I. Stuart and J. H. Levy, *Fuel*, 66 (1987) 493.
- 13 T. Kolyuvec, R. Kuusik and M. Veiderma, *Int. J. Miner. Process.*, 43 (1995) 113.
- 14 V. T. Ciuryla, R. F. Weimer, D. A. Bivans and S. A. Motika, *Fuel*, 58 (1979) 748.
- 15 J. W. Cumming, *Fuel*, 63 (1984) 1436.
- 16 H. Haykiri-Açma, A. Ersoy-Merçboyu and S. Küçükbayrak, *Energy Conversion and Management*, 42 (2001) 11.
- 17 Y. Yürüm, R. Kramer and M. Levy, *Thermochim. Acta*, 94 (1985) 285.
- 18 K. Rajeshwar, *Thermochim. Acta*, 63 (1983) 97.
- 19 D. Thakur and H. E. Nuttall, *Ind. Eng. Chem. Res.*, 26 (1987) 1351.
- 20 J. H. Campbell, G. H. Kosimas, T. T. Caburn and N. D. Stout, *Proc. of the 10th oil shale Symposium*, Colorado School of Mines, Golden, CO 1977.
- 21 O. Dogan and D. Z. Uyzel, *Fuel*, 75 (1996) 1424.
- 22 N. Ahmed and P. T. Williams, *J. Anal. Appl. Pyrol.*, 46 (1998) 31.
- 23 R. A. Haddadin and F. A. Mizyed, *Ind. Eng. Chem. Proc. Des. Dev.*, 13 (1974) 332.
- 24 P. F. V. William, *Fuel*, 64 (1985) 540.
- 25 L. Bilali, K. Elharfi, A. Aouad, M. Benchanâa and A. Mokhlisse, *J. Anal. Appl. Pyrol.*, 65 (2002) 221.
- 26 R. K. Agrawal, *Compositional Analysis by Thermogravimetry*, in C. M. Earnest (Ed.), American Society for Testing and Materials, Philadelphia 1988.
- 27 D. F. Arseneau, *Can. J. Chem.*, 49 (1971) 632.
- 28 A. V. Coats and J. P. Redfern, *Nature*, 201 (1964) 68.
- 29 L. Ballice, M. Yüksel, M. Saglam, H. Schulz and C. Hanoglu, *Fuel*, 74 (1995) 1618.
- 30 H. J. Dembicki, *Org. Geochem.*, 18 (1992) 531.
- 31 I. M. K. Ismail and P. L. Walker, *Fuel*, 68 (1989) 1456.
- 32 B. R. Stanmove, *Fuel*, 70 (1991) 1485.
- 33 M. J. M. Guillena, A. L. Solano and S. M. De Lecea, *Fuel*, 71 (1992) 579.
- 34 A. W. Weitkamp and L. C. Gutberlet, *Ind. Eng. Proc. Des. Dev.*, 9 (1970) 368.